

Pharmacophore Mapping of a Series of 2,4-Diamino-5-deazapteridine Inhibitors of *Mycobacterium avium* Complex Dihydrofolate Reductase

Asim Kumar Debnath[†]

Lindsley F. Kimball Research Institute of the New York Blood Center, 310 East 67th Street, New York, New York 10021

Received July 31, 2001

Pharmacophore hypotheses were developed for a series of 2,4-diamino-5-deazapteridine inhibitors of *Mycobacterium avium* complex (MAC) and human dihydrofolate reductase (hDHFR). Training sets consisting of 20 inhibitors were selected in each case on the basis of the information content of the structures and activity data as required by the HypoGen program in the Catalyst software. In the case of MAC DHFR inhibitors, the best pharmacophore in terms of statistics and predictive value consisted of four features: two hydrogen bond acceptors (HA), one hydrophobic (HY) feature, and one ring aromatic (RA) feature. The selected pharmacophore hypothesis yielded an rms deviation of 0.730 and a correlation coefficient of 0.967 with a cost difference (null cost minus total cost) of approximately 52. The pharmacophore was validated on a large set of test inhibitors. For the test series, a classification scheme was used to distinguish highly active from moderately active and inactive compounds on the basis of activity ranges. This classification scheme is more practical than actual estimated values because these values have no meaning for compounds yet to be tested except that they indicate whether the compounds will be active or inactive in a biological assay. For the training set, the success rate for predicting active and inactive compounds was 100%. For the test set, the success rate in predicting active compounds was greater than 92% while about 7% of the inactive compounds were predicted to be active. This successful prediction was further validated on three structurally diverse compounds active against MAC DHFR. Two compounds mapped well onto three of the four features of the pharmacophore. The third compound was mapped to all four features of the pharmacophore. This validation study provided confidence for the usefulness of the selected pharmacophore model to identify compounds with diverse structures from a database search. Comparison of pharmacophores for inhibitors of human and MAC DHFR is expected to reveal fundamental differences between these two pharmacophores that may be effectively exploited to identify and design compounds with high selectivity for MAC DHFR.

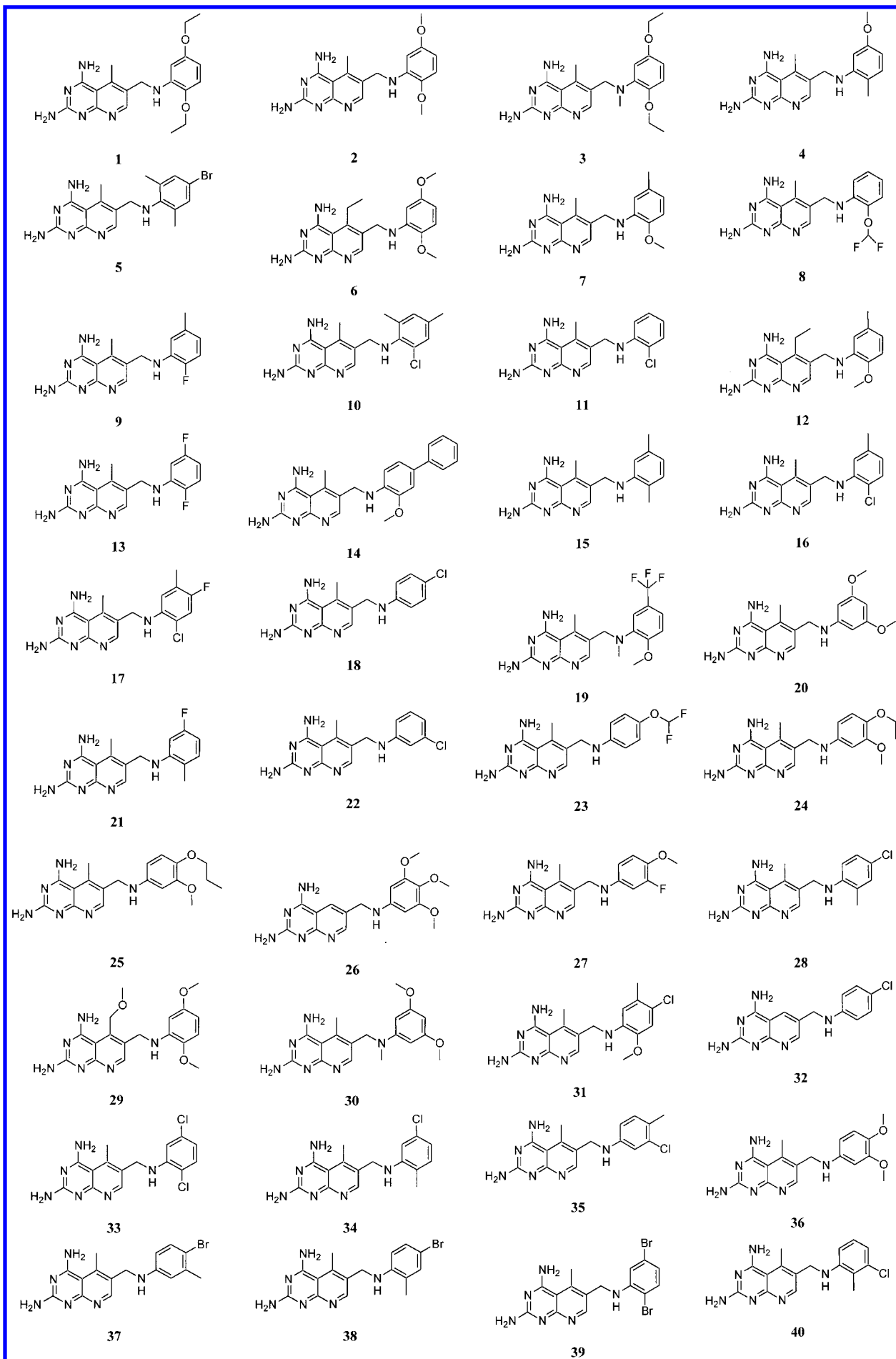
Introduction

Mycobacterium avium complex (MAC),[‡] a group of microorganisms, causes one of the most significant disseminated infections in patients with acquired immunodeficiency syndrome (AIDS).^{1–6} About 50–70% of patients with advanced AIDS are infected with MAC.^{7,8} Infections by MAC in the United States were rare prior to the HIV-1 epidemic. However, at the end of 1999, the Center for Disease Control and Prevention (CDC) reported more than 41 000 cases of infection with MAC. The CD4⁺ cell counts in patients with advanced AIDS may become reduced to below 100, and a correlation has been reported between the CD4⁺ cell count and the development of MAC disease.⁹ These organisms are highly adaptive to their surroundings, e.g., pH and temperature, and are resistant to most antibiotics and available antimycobacterial agents.⁶ Therefore, there is an urgent need to develop antimycobacterial agents targeted to these organisms.

Dihydrofolate reductase (DHFR) is an important enzyme required for the biosynthesis of RNA, DNA, and protein and is the major target of drug development against several diseases, e.g., cancer and bacterial and parasitic infections.^{10–15} It is also one of the best studied enzymes, and the wealth of acquired knowledge is useful for selectively targeting this enzyme to design inhibitors without disrupting the function of the host DHFR. Several reports have been published on the design of MAC DHFR inhibitors.^{16–21} Recently, Suling et al. have reported a large set of deazapteridine derivatives (Figure 1) as potential antimycobacterial agents targeted to MAC DHFR and successfully identified a potent inhibitor with a selectivity index of 2300 [(IC₅₀-(MAC DHFR))/IC₅₀(hDHFR)].¹⁹ We decided to exploit this wealth of information, including the biological activity data, which covers almost a 4 log unit range to develop pharmacophore hypotheses. A pharmacophore represents the three-dimensional (3D) arrangements of chemical features in a molecule (ligand) that may be essential for important binding interactions with a receptor. In the absence of any knowledge of the 3D structure of a receptor, pharmacophores may provide such important information in the drug design process. The pharmacophores may be used in several ways, e.g.,

[†] Phone (212) 570-3373. Fax: (212) 570-3299. E-mail: asim_debnath@nybc.org.

[‡] Abbreviations: MAC, *Mycobacterium avium* complex; DHFR, dihydrofolate reductase; hDHFR, human dihydrofolate reductase; rDHFR, recombinant dihydrofolate reductase; 3D, three-dimensional; NCE, new chemical entity; HA, hydrogen bond acceptor; HD, hydrogen bond donor; HY, hydrophobic; RA, ring aromatic.



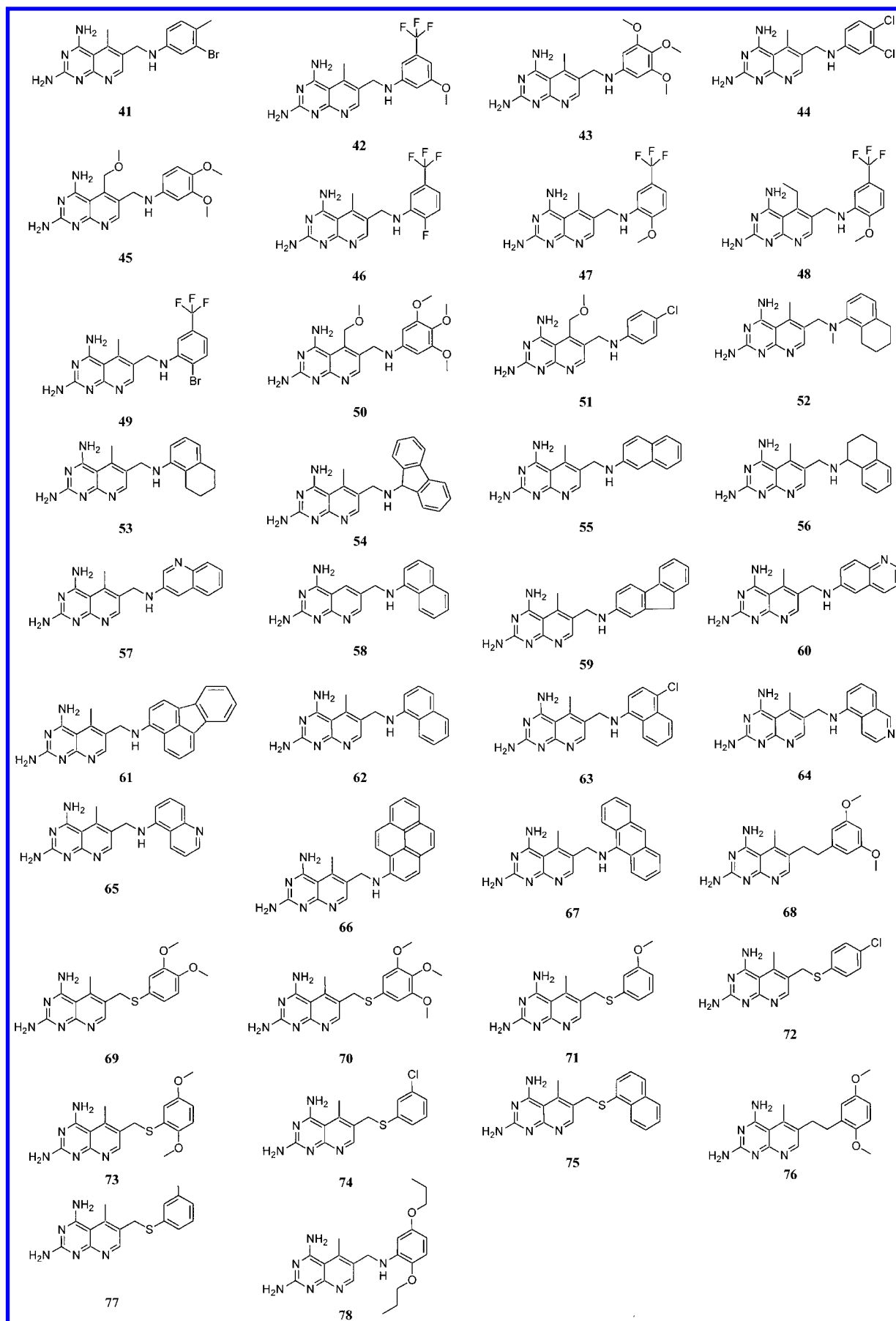


Figure 1. Chemical structures of 2,4-diamino-5-deazapteridines. All structures were drawn using ChemDraw 6.0 software.⁵⁶

as a 3D query in searching 3D databases containing "druglike" small organic molecules to identify active and specific inhibitors or in evaluating a new compound for mapping on a known pharmacophore. The concepts of pharmacophore, their development techniques, and applications have been elegantly compiled in a recently published book.²² This approach is powerful and found wide applications in drug design.^{22–27} A drug discovery cycle, to identify, optimize, and eventually take a compound to the market, is generally a long process (approximately 12–15 years) and is very expensive (approximately \$500 million R&D expense).²⁸ Therefore, there is a pressing need to reduce the cost of drug discovery steps. Pharmaceutical companies are taking more rational approaches than trial and error to identify new chemical entities (NCE). The hypothesis generation methods (HipHop and HypoGen) of the Catalyst software²⁹ have been successfully used in drug discovery research^{30–54} and toxicology⁵⁵ (for a more comprehensive reference lists see http://www.accelrys.com/references/rdd_pub.html). Kaminski et al. reported the development of pharmacophore models from a series of farnesyl protein transferase (FPT) inhibitors.³⁴ The best-derived pharmacophore model was used to search a 3D database from the Schering-Plough Research Institute and successfully identified several low micromolar FPT inhibitors with varied structures compared to the structures used in the training set to develop the pharmacophore. Sprague³⁵ used this method in developing pharmacophores for inhibitors against angiotensin converting enzymes (ACE), protein farnesyl transferase (PFT), human immunodeficiency virus (HIV) protease, and HIV reverse transcriptase (RT). Recently, Kurogi et al. have used Catalyst/HipHop generated pharmacophore in searching 3D database to identify novel mesangial cell proliferation inhibitors.⁵¹ These studies suggest that the Catalyst generated pharmacophores can be effectively used for rational drug design.

Manetti et al. have recently reported the use of the Catalyst/HipHop modules to develop common feature hypotheses for a series of novel antibacterial compounds against both *Mycobacterium tuberculosis* and *Mycobacterium avium* 103317.⁴² We present in this report the development of pharmacophores of a large dataset of antimycobacterial compounds against *Mycobacterium avium* DHFR by using the Catalyst/HypoGen module. Because there is, so far, no report on developing pharmacophores using inhibitors of *Mycobacterium avium* DHFR, this study is expected to provide useful knowledge for developing antimycobacterial drugs targeted to MAC DHFR.

Materials and Methods

Molecular Modeling. All molecular modeling works were performed on a Silicon Graphics Octane² R12000 computer running Irix 6.5.12 (SGI, 1600 Amphitheatre Parkway, Mountain View, CA 94043). Catalyst 4.6 software²⁹ was used to generate pharmacophore models.

Biological Data. Antimycobacterial activities of 2,4-diamino-5-deazapteridines against both MAC and human recombinant DHFR (rDHFR) were taken from the literature¹⁹ and are listed in Tables 1, 3, and 5. Pharmacophore models have been developed using datasets from both systems. The datasets are divided into a training set and a test set. The training sets were selected in such a way so that there was no redundancy in information content in terms of both structural features and

activity ranges. The most active compounds were included so that they provide critical information on pharmacophore requirements. Several moderately active and some inactive compounds were also included to spread the activity ranges as widely as possible. The important aspect of this selection scheme is that each active compound should teach something new to the HypoGen module to help it uncover as much critical information as possible for predicting biological activity. In case of the MAC DHFR system, a training set of 20 compounds with the above criteria has been selected (Table 1); the other 58 compounds were used as the test set (Table 5). Similarly, a training set for the human DHFR system was also selected consisting of 20 compounds (Table 3), and the other 57 compounds were used as the test set (Table 5). An uncertainty value of 3 (default) was used for compound activity, which is a ratio range of uncertainty in the activity value. The activities (IC₅₀) against MAC DHFR have been classified as follows: highly active (<10 nM), moderately active (>10–100 nM), and inactive (>100 nM). The activities against hDHFR have been classified as highly active (<100 nM), moderately active (>100–1000 nM), and inactive (>1000 nM). These activities are classified, somewhat arbitrarily, on the basis of the lowest and the highest activity ranges for each target DHFR enzyme.

Pharmacophore Mapping. Details of the pharmacophore development procedures have been described in the literature.^{22,35} In brief, conformational models of all training set molecules for both MAC DHFR and hDHFR datasets were generated using the "best quality" conformational search option in Catalyst using a constraint of 20 kcal mol⁻¹ energy threshold above the global energy minimum and Charmm force field parameters.⁵⁷ A maximum of 250 conformations were generated to ensure maximum coverage in the conformational space. All other settings were kept as default. Instead of using just the lowest energy conformation of each compound, all conformational models for molecules in each training set were used in Catalyst for pharmacophore hypothesis generation. An initial analysis revealed that four chemical feature types such as hydrogen bond acceptor (HA), hydrogen bond donors (HD), and hydrophobic (HY) and ring aromatic (RA) features could effectively map all critical chemical features of all molecules in the training and test sets. These four feature types were used to generate 10 pharmacophores from both training sets. The Catalyst software can generate pharmacophore hypotheses consisting of a maximum of five features.

Important Output Parameters That Determine the Quality of Pharmacophore Hypothesis. The HypoGen module in Catalyst performs two important theoretical cost calculations (represented in bit units) that determine the success of any pharmacophore hypothesis. One is known as the "fixed cost", which represents the simplest model that fits all data perfectly, and the second one is known as "null cost", which represents the highest cost of a pharmacophore with no features and which estimates activity to be the average of the activity data of the training set molecules. A meaningful pharmacophore hypothesis may result when the difference between these two values is large; a value of 40–60 bits for a pharmacophore hypothesis may indicate that it has 75–90% probability of correlating the data (Catalyst 4.6 documentation). The total cost of any pharmacophore hypothesis should be close to the fixed cost to provide any useful models. Two other parameters that also determine the quality of any pharmacophore hypothesis with possible predictive values are the configuration cost, which is also known as the entropy cost and depends on the complexity of the pharmacophore hypothesis space, and the error cost, which is dependent on the rms differences between the estimated and the actual activities of the training set molecules. The rms deviations represent the quality of the correlation between the estimated and the actual activity data.

Results and Discussions

Pharmacophores have been generated using a set of 20 2,4-diamino-5-deazapteridine derivatives with antimycobacterial activity against both MAC DHFR and

hDHFR. Though the activities of these inhibitors against hDHFR were determined to define the selectivity of inhibitors against MAC DHFR, we have generated pharmacophores for hDHFR inhibitors to understand both the similarities and differences of these pharmacophores that may contribute to selectivity.

1. Mycobacterium Avium Complex DHFR. Pharmacophore Hypothesis Generation. 1.1. Training Set. Sets of 10 hypotheses were generated using the data from 20 training set compounds (Table 1). Different cost values, correlation coefficients (r), rms deviations, and pharmacophore features are listed in Table 2. All 10 hypotheses consist of 4 features. Six of the hypotheses have one hydrogen bond acceptor (HA), one hydrogen bond donor (HD), one hydrophobic (HY) feature, and one ring aromatic (RA) feature, whereas three of the hypotheses have two hydrogen bond donors, one hydrophobic feature, and one ring aromatic feature. The best pharmacophore (hypothesis 1), which has the highest cost difference, lowest error cost, lowest rms difference, and the best correlation coefficient, has two hydrogen bond acceptors, one hydrophobic feature, and one ring aromatic feature. Table 1 shows the actual and estimated antimycobacterial activity of 2,4-diamino-5-deazapteridine derivatives against MAC-DHFR. In the training set compounds, all highly active compounds (<10 nM) were predicted correctly. Two moderately active compounds (>10 – 100 nM) were predicted to be highly active, and all inactive compounds (>100 nM) were correctly predicted to be inactive.

This pharmacophore hypothesis was evaluated for its predictive ability on a large series of test set compounds.

1.2. Test Set. The purpose of the pharmacophore hypothesis generation is not just to predict the activity of the training set compounds accurately but also to verify whether the pharmacophore models are capable of predicting the activities of compounds of test series and classifying them correctly as active or inactive. We have constructed a large set of test set compounds (58), and conformational studies were done as described earlier. The estimated activities were scored using hypothesis 1 as the pharmacophore (Table 5). Out of 55 highly active compounds (<10 nM), 51 were accurately predicted as highly active (92.7% success) and only one highly active compound was predicted as inactive. The model also incorrectly predicted one inactive compound as active, three inactive compounds as moderately active, one moderately active compound as inactive, and one inactive compound as moderately active.

One of the most active as well as most selective antimycobacterial compounds among all the compounds tested in this series (compound no. 1, selectivity ratio of 2300) was selected from the training set to show the mapping of this compound on the selected pharmacophore (hypothesis 1, Figure 2A). This pharmacophore predicted the antimycobacterial activity of this compound against MAC DHFR remarkably well (actual IC_{50} of 0.84 nM vs the estimated activity of 0.90 nM). To give some indications of how well the active compounds from the test set mapped this pharmacophore, one of the most active compounds (no. 65) has been selected and mapped on this pharmacophore and is shown in Figure 2B. This compound mapped the pharmacophore very well, and the estimated activity, calculated on the basis of this

pharmacophore, was close to the actual activity (actual IC_{50} of 0.98 nM vs the estimated value of 0.97 nM) and is shown as +++ in Table 5. Both these compounds mapped all four important features very well. Inactive compounds either missed one or more features, or some structural portion of the compound was outside the pharmacophore features. Out of 58 test set compounds only 4 inactive compounds ($<7\%$) mapped the pharmacophore correctly and gave false positive results.

2. Human DHFR. Pharmacophore Hypothesis Generation. 2.1. Training Set. A training set of 20 compounds tested against human DHFR (Table 3) was used to develop pharmacophore hypotheses. A total of 10 hypotheses were generated (Table 4) using the same criteria as were used for MAC DHFR inhibitors. The details of the hypotheses are shown in Table 4. Overall, hypothesis 1 has the best statistical significance in terms of its predictive ability, as indicated by the high correlation coefficient and low rms deviations (Table 4). The total cost (88.167 bits) is close to the fixed cost (83.088 bits), and also a high cost difference (~ 52 bits) is indicative of greater predictability of the pharmacophore model. This pharmacophore hypothesis has three hydrogen bond donating features and one hydrophobic feature, which contrasts sharply with the best pharmacophore hypothesis obtained with the training set compounds against MAC DHFR. This pharmacophore model has been used to estimate the activity of the compounds in the training set (Table 3). Out of 10 highly active compounds ($IC_{50} < 100$ nM), all were predicted to be highly active (100% success). Out of six moderately active compounds ($IC_{50} > 100$ – 1000 nM), all but one were predicted correctly. All four inactive compounds ($IC_{50} > 1000$ nM) were also predicted correctly. One moderately active compound was estimated to be inactive.

2.2. Test Set. A total of 57 compounds with activity data were selected as test set compounds. Hypothesis 1 was selected as the best model and was used to estimate their activity (Table 5), represented again as follows: +++, highly active; ++, moderately active; +, inactive. A total of 30 of 33 highly active compounds were predicted to be highly active ($\sim 91\%$ success); the other three were predicted to be moderately active. A total of 6 out of 15 moderately active compounds were predicted correctly, whereas 8 were predicted to be highly active and one inactive. A total of 2 inactive compounds out of 9 were predicted correctly, but 4 were predicted to be highly active and the other 3 were predicted to be moderately active. The success rate in classifying active compounds as active is very similar to that obtained by the selected pharmacophore generated against MAC DHFR inhibitors. But the pharmacophore for human DHFR performed poorly in predicting inactive compounds correctly.

This poor performance can probably be explained by the fact that all the inactive compounds against human DHFR have long-chain or bulky alkyl groups at the R_1 , R_2 , and R_5 positions (Figure 1), e.g., $-\text{CH}_2\text{OCH}_3$ at position R_1 (compound no. 29, $IC_{50} = 31\,000$ nM) and $-\text{OCH}_2\text{CH}_3$ (compound no. 1, $IC_{50} = 2300$ nM; compound no. 3, $IC_{50} = 1000$ nM) and $-\text{O}(\text{CH}_2)_2\text{CH}_3$ (compound no. 78, $IC_{50} = 7300$ nM) at both R_2 and R_5 positions. It is important to note that the Catalyst

Table 1. Training Set Molecules Used To Develop Pharmacophore Hypotheses for MAC DHFR

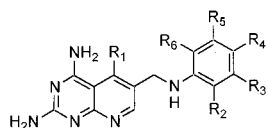
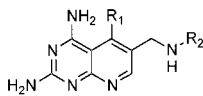
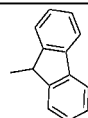
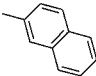
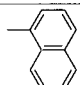
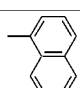
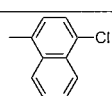
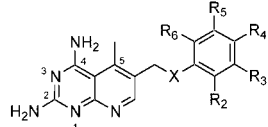
Number	Molecule No.							MAC DHFR IC ₅₀ (nM)	
		R ₁	R ₂	R ₃	R ₄	R ₅	R ₆	Actual	Estimated based on Hypothesis- 1
1	1	CH ₃	OCH ₂ CH ₃	H	H	OCH ₂ CH ₃	H	0.84	0.90
2	26	H	H	OCH ₃	OCH ₃	OCH ₃	H	240	560
3	28	CH ₃	CH ₃	H	Cl	H	H	0.19	0.41
4	29	CH ₂ OCH ₃	OCH ₃	H	H	OCH ₃	H	2400	590
5	44	CH ₃	H	Cl	Cl	H	H	0.92	1.1
6	45	CH ₂ OCH ₃	H	OCH ₃	OCH ₃	H	H	1200	490
7	50	CH ₂ OCH ₃	H	OCH ₃	OCH ₃	OCH ₃	H	550	540
8	51	CH ₂ OCH ₃	H	H	Cl	H	H	1500	370
									
		R ₁		R ₂					
9	54	CH ₃						320	170
10	55	CH ₃						0.76	0.93
11	58	H						86	440
12	62	CH ₃						0.81	1.4
13	63	CH ₃						0.43	1.3
									
		X	R ₂	R ₃	R ₄	R ₅	R ₆		
14	68	CH ₂	H	OCH ₃	H	OCH ₃	H	1.5	1.5
15	72	S	H	H	Cl	H	H	3.6	5.6
16	73	S	OCH ₃	H	H	OCH ₃	H	23	8.5
17	75	S	1-Naphthyl					4.6	6.4
18	76	CH ₂	OCH ₃	H	H	OCH ₃	H	47	54
19	77	S	H	H	H	CH ₃	H	16	6.1
20	78	NH	O(CH ₂) ₂ CH ₃	H	H	O(CH ₂) ₂ CH ₃	H	1	1.2

Table 2. Results of Pharmacophore Hypotheses Generated Using Training Set Molecules against MAC DHFR

hypothesis no. ^a	total cost	cost difference (null cost – total cost)	error cost	rms	correlation (<i>r</i>)	features ^b
1	90.856	51.820	72.606	0.730	0.967	HA, HA, HY, RA
2	91.542	51.134	74.874	0.872	0.950	HA, HD, HY, RA
3	92.091	50.585	73.457	0.786	0.962	HA, HD, HY, RA
4	92.260	50.416	76.397	0.955	0.938	HD, HD, HY, RA
5	92.416	50.260	75.741	0.920	0.943	HD, HD, HY, RA
6	93.014	49.662	75.527	0.908	0.946	HA, HD, HY, RA
7	93.073	49.603	75.678	0.917	0.945	HA, HD, HY, RA
8	94.374	48.302	75.671	0.916	0.947	HA, HD, HY, RA
9	94.693	47.983	78.589	1.064	0.922	HD, HD, HY, RA
10	94.729	47.947	77.036	0.988	0.936	HA, HD, HY, RA

^a Null cost = 142.676. Fixed cost = 82.566. Configuration = 14.169. All cost units are in bits. ^b HA, hydrogen bond acceptor; HD, hydrogen bond donor; HY, hydrophobic feature; RA, ring aromatic feature.

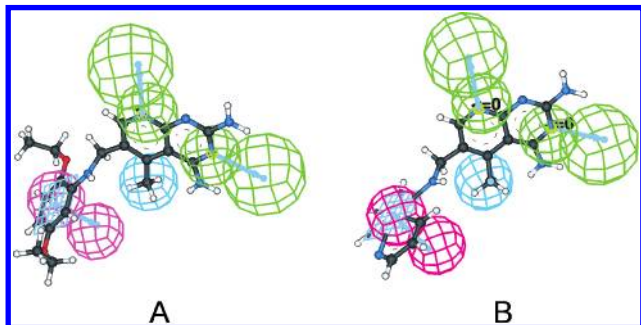


Figure 2. Mapping of two of the most active compounds, (A) compound no. 1 from the training set and (B) compound no. 65 from the test set on the selected pharmacophore (hypothesis 1) developed against MAC DHFR inhibitors. The green, blue, and pink contours represent the hydrogen bond accepting feature (HA), hydrophobic feature (HY), and ring aromatic feature (RA), respectively.

program is not capable of handling any steric effect that might be responsible for the lower activity of any compound. All the above compounds, except compound no. 29, are highly active against MAC DHFR. This analysis indicates that the binding site on the human DHFR is most likely much more compact than that of the MAC DHFR. In the absence of any 3D structure of MAC DHFR, this observation could not be verified.

Two of the most active compounds, one each from the training (compound no. 62) and the test set (compound no. 47), were mapped on the pharmacophore (hypothesis 1) and are shown in parts A and B of Figure 3, respectively. These two active compounds have substantial structural differences but mapped remarkably well on the selected pharmacophore, and the activities were predicted well by the pharmacophore. The most active training set compound (no. 62) has an IC_{50} value of 2 nM, and this model estimated its activity as 5.9 nM. Similarly, one of the most active compounds in the test set (no. 47) has an IC_{50} value of 2.7 nM, and this model estimated the activity as 6.5 nM. Therefore, it appears that the highly active compounds inhibiting human DHFR mapped well onto the selected pharmacophore.

3. Validation of the Pharmacophore Generated from MAC DHFR Inhibitors on Three Structurally Diverse Classes of Compounds That Show Activity against MAC DHFR. One of the goals of pharmacophore generation is to identify active compounds from a 3D database that are structurally different and diverse. To get additional confidence on the usefulness of the pharmacophore model we generated from MAC DHFR inhibitors, we validated the model by mapping

three structurally diverse classes of compounds (Figure 4), active against MAC DHFR, which were reported by three different research groups (Figure 5). We did not attempt to compare the actual experimental activity with the estimated activity by the pharmacophore model because the assay systems used by different research groups were not identical. The mapping information based on the pharmacophores we developed may help to modify existing molecules from the three series of compounds to develop drugs with better antimycobacterial activity.

In 1999, Rosowsky et al. reported the antiparasitic activities against DHFR, including MAC DHFR, of a series of 2,4-diaminopteridines with bridged diarylamine side chains.²¹ The most potent (IC_{50} = 0.012 μ M) and selective analogue, *N*-[(2,4-diaminopteridine-6-yl)-methyl]dibenz[*b,f*]azepine (Figure 4A), was mapped on the pharmacophore (Figure 5A) after a conformational study using the “best” option in Catalyst. The 2,4-diaminopteridine moiety of this compound mapped similarly to the training and test series; i.e., the two hydrogen bond acceptor features (HA) mapped correctly on two of the nitrogen atoms. The hydrophobic feature (HY) mapped on one of the phenyl groups of the dibenz[*b,f*]azepine ring. However, the molecule failed to map on the ring aromatic (RA) feature of the pharmacophore. Therefore, out of four features in the generated pharmacophore, the compound satisfied three features. This may explain the low micromolar activity of this compound. Nevertheless, the mapping clearly shows that the bridged side chain needs further modification to map correctly onto the ring aromatic feature, and this information may help in designing compounds with improved activity.

Meyer et al. in 1995 reported the inhibitory activity of a dihydrofolate reductase inhibitor, 4,6-diamino-1,2-dihydro-2,2-dimethyl-1-[(2,4,5-trichlorophenoxy)propyloxy]-1,3,5-triazine hydrobromide (WR99210), against the *Mycobacterium avium* complex¹⁶ (Figure 4B). A conformational analysis was initiated as before, and then all conformers of the compound were mapped on the pharmacophore. Out of two hydrogen bond acceptor features (HA), one mapped on one of the nitrogen atoms of the dihydrotriazine ring; the hydrophobic (HY) and ring aromatic (RA) features mapped quite well on one of the methyl groups on the triazine ring and the dichloro-substituted phenyl ring, respectively (Figure 5B). In this case, again three out four features mapped quite well and indicated room for chemical modification for further improvement of activity.

Table 3. Training Set Molecules Used To Develop Pharmacophore Hypotheses against hDHFR

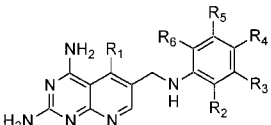
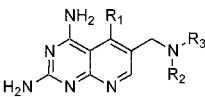
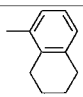
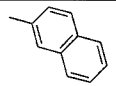
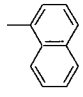
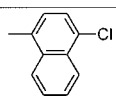
Number	Molecule No.							h-DHFR IC ₅₀ (nM)	
		R ₁	R ₂	R ₃	R ₄	R ₅	R ₆	Actual	Estimated
									(based on Hypothesis- 1)
1	18	CH ₃	H	H	Cl	H	H	27	6.9
2	20	CH ₃	H	OCH ₃	H	OCH ₃	H	15	11
3	23	CH ₃	H	H	OCHF ₂	H	H	20	5.9
4	26	H	H	OCH ₃	OCH ₃	OCH ₃	H	3900	3900
5	29	CH ₂ OCH ₃	OCH ₃	H	H	OCH ₃	H	31000	8000
6	36	CH ₃	H	OCH ₃	OCH ₃	H	H	5.1	13
7	41	CH ₃	H	Br	CH ₃	H	H	3.7	7
8	43	CH ₃	H	OCH ₃	OCH ₃	OCH ₃	H	4.7	11
9	45	CH ₂ OCH ₃	H	OCH ₃	OCH ₃	H	H	6100	5900
10	51	CH ₂ OCH ₃	H	H	Cl	H	H	2600	3300
									
		R ₁	R ₂	R ₃					
11	52	CH ₃	CH ₃				710	670	
12	55	CH ₃	H				10	6.1	
13	58	H	H				820	1100	
14	63	CH ₃	H				2.0	5.9	

Table 3 (Continued)

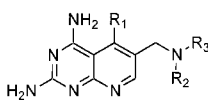
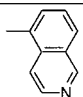
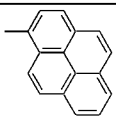
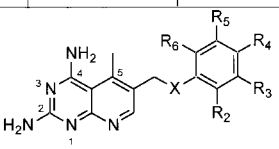
									
		R ₁	R ₂	R ₃					
15	64	CH ₃	H		4.0	6.3			
16	66	CH ₃	H		3.8	6.2			
									
		X	R ₂	R ₃	R ₄	R ₅	R ₆		
17	68	CH ₂	H	OCH ₃	H	OCH ₃	H	990	640
18	72	S	H	H	Cl	H	H	590	660
19	75	S	1-Naphthyl					440	670
20	77	S	H	H	H	CH ₃	H	850	670

Table 4. Results of Pharmacophore Hypotheses Generated Using Training Set Molecules against hDHFR

hypothesis no.	total cost	cost difference (null cost ^a – total cost)	error cost	rms	correlation (r)	features ^b
1	88.167	51.931	71.301	0.635	0.973	HD, HD, HD, HY
2	88.547	51.551	72.031	0.690	0.967	HD, HD, HD, HY
3	88.858	51.240	72.253	0.706	0.965	HA, HD, HD, HY
4	89.076	51.022	72.006	0.688	0.968	HD, HD, HY, HY
5	89.498	50.600	72.481	0.722	0.965	HA, HD, HY, HY
6	89.668	50.430	73.345	0.779	0.958	HA, HA, HD, HY
7	89.680	50.418	72.323	0.711	0.966	HD, HD, HY, HY
8	90.050	50.048	72.968	0.755	0.961	HD, HY, HY, RA
9	90.206	49.892	73.488	0.788	0.957	HA, HD, HY, HY
10	90.388	49.710	73.606	0.796	0.956	HA, HD, HY, HY

^a Null cost = 140.098. Fixed cost = 83.088. Configuration = 14.691. All cost units are in bits. ^b HA, hydrogen bond acceptor; HD, hydrogen bond donor; HY, hydrophobic feature; RA, ring aromatic feature.

In 1998, Ganjee et al. reported activities of a series of conformationally restricted tetrahydropyrido-annulated furo[2,3-*d*]pyrimidines against dihydrofolate reductase from several organisms, including the *Mycobacterium avium* complex.²⁰ One of the compounds, 2,4-diamino-5,6,7,8-tetrahydro-7-(4'-benzoyl-L-glutamic acid)-pyrido[4',3':4,5]furo[2,3-*d*]pyrimidine (Figure 4C), showed the highest potency (IC₅₀ = 0.97 μM) among all the compounds tested. A conformational analysis was carried out as before, and all the conformers were mapped on the pharmacophore. This compound successfully mapped on all four features of the selected MAC DHFR pharmacophore. The carbonyl group in one of the carboxylic acids and the carbonyl group in the L-

glutamic acid moiety mapped on the hydrogen bond acceptor features, the phenyl group mapped to the hydrophobic feature, and the furan ring mapped onto the ring aromatic feature (Figure 5C).

This validation study provides additional confidence for the pharmacophore models and suggests that they may help in identifying, in a 3D database search, structurally diverse compounds with potent and selective inhibitory activity against MAC DHFR.

Conclusions

The work presented in this study shows how chemical features of a set of compounds along with their activities ranging over several orders of magnitudes can be used

Table 5. Experimental Inhibitory Activity and Activity Scale (Assigned and Estimated) of Test Set Molecules Using Hypothesis 1 from Tables 2 and 4 against MAC DHFR and hDHFR, Respectively

molecule no.	antimycobacterial activity against MAC-DHFR			antimycobacterial activity against h-DHFR activity		
	exptl IC ₅₀ (nM)	activity scale ^a	estimated activity scale	exptl IC ₅₀ (nM)	activity scale ^b	estimated activity scale
1				2300	+	+++
2	1.1	+++	+++	1000	++	+++
3	1.4	+++	+++	1000	++	++
4	0.4	+++	+++	150	++	+++
5	5.3	+++	+	1900	+	+
6	2.8	+++	++	1000	++	++
7	0.86	+++	+++	300	++	+++
8	0.87	+++	+++	277	++	+++
9	1.1	+++	+++	250	++	+++
10	3.8	+++	+++	850	++	+++
11	0.91	+++	+++	120	++	+++
12	3.1	+++	+++	370	++	++
13	0.9	+++	+++	69	+++	+++
14	0.91	+++	+++	68	+++	+++
15	0.92	+++	+++	57	+++	+++
16	0.95	+++	+++	44	+++	+++
17	0.78	+++	+++	33	+++	+++
18	0.84	+++	+++			
19	1.2	+++	++	36	+++	++
20	0.64	+++	+++			
21	0.85	+++	+++	19	+++	+++
22	0.82	+++	+++	17	+++	+++
23	1.1	+++	+++			
24	1.1	+++	+++	18	+++	+++
25	0.93	+++	+++	15	+++	+++
26						
27	0.91	+++	+++	14	+++	+++
28				2.8	+++	+++
29						
30	0.73	+++	+++	8.7	+++	++
31	0.94	+++	+++	10	+++	+++
32	73	++	+	670	++	+
33	0.89	+++	+++	8	+++	+++
34	0.79	+++	+++	6.1	+++	+++
35	0.9	+++	+++	6.7	+++	+++
36	0.7	+++	+++			
37	0.87	+++	+++	6.1	+++	+++
38	0.85	+++	+++	5.9	+++	+++
39	0.7	+++	+++	4.6	+++	+++
40	0.82	+++	+++	5.2	+++	+++
41	0.6	+++	+++			
42	0.93	+++	+++	5.5	+++	+++
43	0.82	+++	+++			
44				5	+++	+++
45						
46	0.86	+++	+++	4.1	+++	+++
47	0.66	+++	+++	2.7	+++	+++
48	0.88	+++	+++	3.6	+++	++
49	0.82	+++	+++	3.2	+++	+++
50				1300	+	+
51						
52	1.9	+++	++			
53	0.93	+++	+++	142	++	+++
54				5300	+	+++
55						
56	280	+	++	3400	+	+++
57	1.2	+++	+++	12	+++	+++
58						
59	0.86	+++	+++	6.7	+++	+++
60	0.95	+++	+++	7.1	+++	+++
61	1	+++	+++	6.2	+++	+++
62				4.3	+++	+++
63						
64	0.87	+++	+++			
65	0.98	+++	+++	4.3	+++	+++
66	0.88	+++	+++			
67	620	+	+++			
68						
69	1.5	+++	+++	440	++	++
70	4.5	+++	+++	1200	+	++
71	2.7	+++	+++	500	++	++
72						
73				2500	+	++

Table 5 (Continued)

molecule no.	antimycobacterial activity against MAC-DHFR			antimycobacterial activity against hDHFR activity		
	exptl IC ₅₀ (nM)	activity scale ^a	estimated activity scale	exptl IC ₅₀ (nM)	activity scale ^b	estimated activity scale
74	3.9	+++	+++	420	++	++
75						
76				2700	+	++
77						
78				7300	+	+++

^a MAC DHFR activity scale: +++, <10 nM (highly active); ++, >10–100 nM (moderately active); +, >100 nM (inactive). ^b h-DHFR activity scale: +++, <100 nM (highly active); ++, >100–1000 nM (moderately active); +, >1000 nM (inactive).

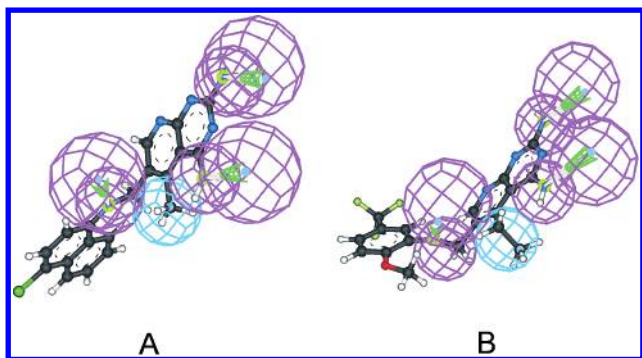


Figure 3. Mapping of two of the most active compounds, (A) compound no. 62 from the training set and (B) compound no. 47 from the test set on the selected pharmacophore (hypothesis 1) developed against human DHFR inhibitors. The violet and blue contours represent the hydrogen bond donating feature (HD) and the hydrophobic feature (HY), respectively.

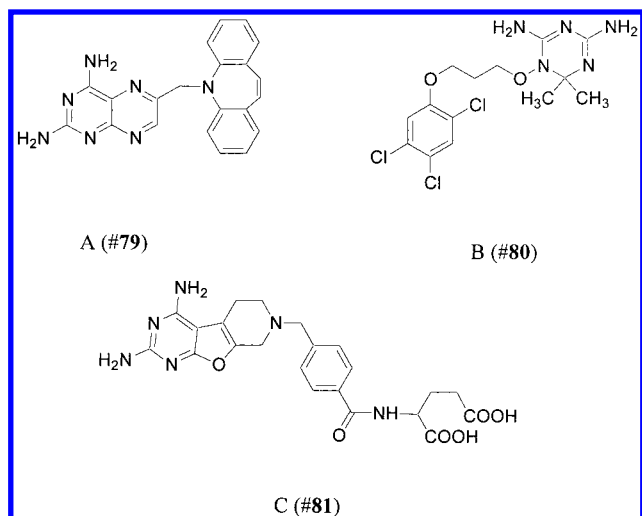


Figure 4. Chemical structures of three diverse MAC DHFR inhibitors used for the validation study: (A) *N*-[(2,4-diaminopteridine-6-yl)methyl]dibenz[*b,f*]azepine (no. 79); (B) 4,6-diamino-1,2-dihydro-2,2-dimethyl-1-[(2,4,5-trichlorophenoxy)propyloxy]-1,3,5-triazine hydrobromide (no. 80); (C) 2,4-diamino-5,6,7,8-tetrahydro-7-(4'-benzoyl-L-glutamic acid)pyrido[4',3':4,5]furo[2,3-*d*]pyrimidine (no. 81).

to generate pharmacophore hypotheses that can successfully predict the activity. The models were not only predictive within the same series of compounds but three different classes of diverse compounds also effectively mapped onto most of the features important for activity. The pharmacophores generated from MAC DHFR inhibitors can be used (1) as a three-dimensional query in database searches to identify compounds with diverse structures that can potentially inhibit MAC DHFR selectively and (2) to evaluate how well any newly designed compound maps on the pharmacophore

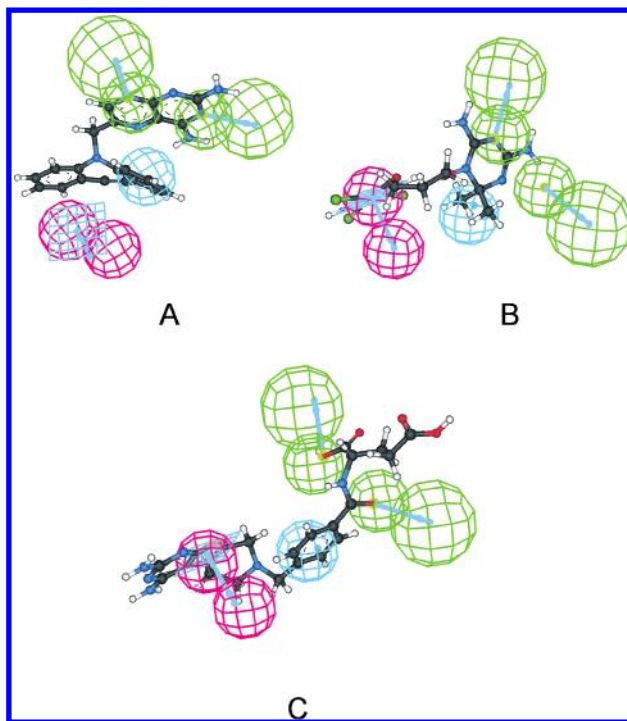


Figure 5. Mapping of compound nos. 79–81 on the selected pharmacophore (hypothesis 1) developed against MAC DHFR inhibitors. The color contours have the same annotation as for Figure 2.

before undertaking any further study including synthesis. Both these applications may help in identifying or designing compounds for further biological evaluation and optimization.

The pharmacophores developed in this study using inhibitors against *Mycobacterium avium* complex and human DHFR showed distinct chemical features that may be responsible for the activity of the inhibitors. The knowledge concerning the differences in pharmacophore patterns of these two systems is expected to be useful in identifying and designing inhibitors with greater selectivity toward the MAC DHFR. We intend to utilize the information to undertake 3D searches on large databases of druglike molecules to identify a new generation of MAC DHFR inhibitors.

Acknowledgment. I thank Drs. A. Robert Neurath and Cynthia Selassie for thoroughly reading the manuscript and their critical comments. This work was supported by grants from NIH (Grant AI46221, A.K.D. Co-PI), Phillip Morris, Inc., and Johnson & Johnson.

References

- Schurmann, D.; Nightingale, S. D.; Bergmann, F.; Ruf, B. Tuberculosis and HIV infection: a review. *Infection* **1997**, *25*, 274–280.

- (2) Benson, C. Disseminated *Mycobacterium avium* complex disease in patients with AIDS. *AIDS Res. Hum. Retroviruses* **1994**, *10*, 913–916.
- (3) Churchyard, G. J.; Grant, A. D. HIV infection, tuberculosis and non-tuberculous mycobacteria. *S. Afr. Med. J.* **2000**, *90*, 472–476.
- (4) Mary-Krause, M.; Rabaud, C.; Jouan, M.; Obadia, M.; de la Blanchardiere, A.; Raffi, F.; May, T. *Mycobacterium avium* complex disease in HIV seropositive patients: incidence and risk factors before and after the introduction of highly active anti-retroviral treatments. Clinical Epidemiology Group of the Information and Care Center for Human Immunodeficiency. *Pathol. Biol.* **2000**, *48*, 495–504.
- (5) Ghassemi, M.; Andersen, B. R.; Reddy, V. M.; Gangadharam, P. R.; Spear, G. T.; Novak, R. M. Human immunodeficiency virus and *Mycobacterium avium* complex coinfection of monocytoïd cells results in reciprocal enhancement of multiplication. *J. Infect. Dis.* **1995**, *171*, 68–73.
- (6) Reddy, V. M. Mechanism of *Mycobacterium avium* complex pathogenesis. *Front. Biosci.* **1998**, *3*, d525–d531.
- (7) Barrow, W. W. Processing of mycobacterial lipids and effects on host responsiveness. *Front. Biosci.* **1997**, *2*, d387–d400.
- (8) Horsburgh, C. R., Jr. *Mycobacterium avium* complex infection in the acquired immunodeficiency syndrome. *N. Engl. J. Med.* **1991**, *324*, 1332–1338.
- (9) Nightingale, S. D.; Byrd, L. T.; Southern, P. M.; Jockusch, J. D.; Cal, S. X.; Wynne, B. A. Incidence of *Mycobacterium avium-intracellulare* complex bacteremia in human immunodeficiency virus-positive patients. *J. Infect. Dis.* **1992**, *165*, 1082–1085.
- (10) Milne, G. W.; Wang, S.; Nicklaus, M. C. Molecular modeling in the discovery of drug leads. *J. Chem. Inf. Comput. Sci.* **1996**, *36*, 726–730.
- (11) Jacobson, M. A.; French, M. Altered natural history of AIDS-related opportunistic infections in the era of potent combination antiretroviral therapy. *AIDS* **1998**, *12* (Suppl. A), S157–S163.
- (12) Rastogi, N.; Potar, M. C.; David, H. L. Action of antituberculous and beta-lactam drugs (including imipenem) against extra- and intra-cellularly growing *Mycobacterium avium-intracellulare*. *Ann. Inst. Pasteur/Microbiol.* **1988**, *139*, 225–232.
- (13) Ekins, S.; Bravi, G.; Binkley, S. A.; Gillespie, J. S.; Ring, B. J.; Wikel, J. H.; Wrighton, S. A. Three- and four-dimensional quantitative structure activity relationship analyses of cytochrome P-450 3A4 inhibitors. *J. Pharmacol. Exp. Ther.* **1999**, *290*, 429–438.
- (14) Hessel, N. A.; Schwarcz, S.; Ameli, N.; Oliver, G.; Greenblatt, R. M. Accuracy of self-reports of acquired immunodeficiency syndrome and acquired immunodeficiency syndrome-related conditions in women. *Am. J. Epidemiol.* **2001**, *153*, 1128–1133.
- (15) Marquez-Diaz, F.; Soto-Ramirez, L. E.; Sifuentes-Osorio, J. Nocardiosis in patients with HIV infection. *AIDS Patient. Care STDs.* **1998**, *12*, 825–832.
- (16) Meyer, S. C.; Majumder, S. K.; Cynamon, M. H. In vitro activities of PS-15, a new dihydrofolate reductase inhibitor, and its cyclic metabolite against *Mycobacterium avium* complex. *Antimicrob. Agents Chemother.* **1995**, *39*, 1862–1863.
- (17) Suling, W. J.; Reynolds, R. C.; Barrow, E. W.; Wilson, L. N.; Piper, J. R.; Barrow, W. W. Susceptibilities of *Mycobacterium tuberculosis* and *Mycobacterium avium* complex to lipophilic deazapteridine derivatives, inhibitors of dihydrofolate reductase. *J. Antimicrob. Chemother.* **1998**, *42*, 811–815.
- (18) Shoen, C. M.; Choromanska, O.; Reynolds, R. C.; Piper, J. R.; Johnson, C. A.; Cynamon, M. H. In vitro activities of several diaminomethylpyridopyrimidines against *Mycobacterium avium* complex. *Antimicrob. Agents Chemother.* **1998**, *42*, 3315–3316.
- (19) Suling, W. J.; Seitz, L. E.; Pathak, V.; Westbrook, L.; Barrow, E. W.; Zywno-Van-Ginkel, S.; Reynolds, R. C.; Piper, J. R.; Barrow, W. W. Antimycobacterial activities of 2,4-diamino-5-deazapteridine derivatives and effects on mycobacterial dihydrofolate reductase. *Antimicrob. Agents Chemother.* **2000**, *44*, 2784–2793.
- (20) Gangjee, A.; Elzein, E.; Queener, S. F.; McGuire, J. J. Synthesis and biological activities of tricyclic conformationally restricted tetrahydropyrido annulated furo[2,3-d]pyrimidines as inhibitors of dihydrofolate reductases. *J. Med. Chem.* **1998**, *41*, 1409–1416.
- (21) Rosowsky, A.; Cody, V.; Galitsky, N.; Fu, H.; Papoulis, A. T.; Queener, S. F. Structure-based design of selective inhibitors of dihydrofolate reductase: synthesis and antiparasitic activity of 2,4-diaminopteridine analogues with a bridged diarylamine side chain. *J. Med. Chem.* **1999**, *42*, 4853–4860.
- (22) *Pharmacophore Perception, Development, and Use in Drug Design*; Güner, O. F., Ed.; International University Line: La Jolla, CA 2000.
- (23) Martin, Y. C. Pharmacophore mapping. In *Designing Bioactive Molecules: Three-Dimensional Techniques and Application*; Martin, Y. C., Willett, P., Eds.; American Chemical Society: Washington, DC, 1998; pp 121–148.
- (24) Clark, D. E.; Westhead, D. R.; Sykes, R. A.; Murray, C. W. Active-site-directed 3D database searching: pharmacophore extraction and validation of hits. *J. Comput. Aided Mol. Des.* **1996**, *10*, 397–416.
- (25) Doweiko, A. M. Three-dimensional pharmacophores from binding data. *J. Med. Chem.* **1994**, *37*, 1769–1778.
- (26) Mason, J. S.; Good, A. C.; Martin, E. J. 3-D pharmacophores in drug discovery. *Curr. Pharm. Des.* **2001**, *7*, 567–597.
- (27) Milne, G. W.; Nicklaus, M. C.; Wang, S. Pharmacophores in drug design and discovery. *SAR QSAR Environ. Res.* **1998**, *9*, 23–38.
- (28) *PhRMA: New Medicines in Development Series*; 2001 (<http://www.phrma.org/publications/documents/factsheets/2001-03-01.210.phtml>).
- (29) *Catalyst*, version 4.6; Accelrys, Inc. (previously known as Molecular Simulations, Inc.): 9685 Scranton Road, San Diego, CA 92121, 2000.
- (30) Greenidge, P. A.; Weiser, J. A comparison of methods for pharmacophore generation with the Catalyst software and their use for 3D-QSAR: Application to a set of 4-aminopyridine thrombin inhibitors. *Mini-Rev. Med. Chem.* **2001**, *1*, 79–87.
- (31) Palomer, A.; Pascual, J.; Cabre, F.; Garcia, M. L.; Mauleon, D. Derivation of pharmacophore and CoMFA models for leukotriene D(4) receptor antagonists of the quinolinyl(bridged)aryl series. *J. Med. Chem.* **2000**, *43*, 392–400.
- (32) Duffy, J. C.; Deardon, J. C.; Green, D. S. V. Use of Catalyst in the design of novel non-steroidal anti-inflammatory analgesic drugs. In *QSAR and Molecular Modelling: Concepts, Computational Tools and Biological Applications*; Sanz, F., Giraldo, J., Manaut, F., Eds.; Prous Science Publishers: Barcelona, 1995; pp 289–291.
- (33) Hoffman, R. D.; Bourguignon, J. J. Building a hypothesis for CCK-B antagonists using Catalyst program. In *QSAR and Molecular Modelling: Concepts, Computational Tools and Biological Applications*; Sanz, F., Giraldo, J., Manaut, F., Eds.; Prous Science Publishers: Barcelona, 1995; pp 298–300.
- (34) Kaminski, J. J.; Rane, D. F.; Snow, M. E.; Weber, L.; Rothofsky, M. L.; Anderson, S. D.; Lin, S. L. Identification of novel farnesyl protein transferase inhibitors using three-dimensional database searching methods. *J. Med. Chem.* **1997**, *40*, 4103–4112.
- (35) Sprague, P. W. Automated chemical hypothesis generation and database searching with Catalyst. In *Perspectives in Drug Discovery and Design*; Müller, K., Eds.; ESCOM Science Publishers B. V.: Leiden, The Netherlands, 1995; pp 1–21.
- (36) Quintana, J.; Contijoch, M.; Cuberes, R.; Frigola, J. Structure-activity relationships and molecular modeling studies of a series of H1 antihistamines. In *QSAR and Molecular Modelling: Concepts, Computational Tools and Biological Applications*; Sanz, F., Giraldo, J., Manaut, F., Eds.; Prous Science Publishers: Barcelona, 1995; pp 282–288.
- (37) Barbaro, R.; Betti, L.; Botta, M.; Corelli, F.; Giannaccini, G.; Maccari, L.; Manetti, F.; Strappaghetti, G.; Corsano, S. Synthesis, biological evaluation, and pharmacophore generation of new pyridazinone derivatives with affinity toward α_1 - and α_2 -adrenoceptors. *J. Med. Chem.* **2001**, *44*, 2118–2132.
- (38) Baringhaus, K. H.; Matter, H.; Stengelin, S.; Kramer, W. Substrate specificity of the ileal and the hepatic Na(+)/bile acid cotransporters of the rabbit. II. A reliable 3D QSAR pharmacophore model for the ileal Na(+)/bile acid cotransporter. *J. Lipid Res.* **1999**, *40*, 2158–2168.
- (39) Ekins, S.; de Groot, M. J.; Jones, J. P. Pharmacophore and three-dimensional quantitative structure activity relationship methods for modeling cytochrome p450 active sites. *Drug Metab. Dispos.* **2001**, *29*, 936–944.
- (40) Hirashima, A.; Rafaei, A.; Gileadi, C.; Kuwano, E. Three-dimensional pharmacophore hypotheses of octopamine receptor responsible for the inhibition of sex-pheromone production in *Helicoverpa armigera*. *J. Mol. Graphics Modell.* **1999**, *17*, 43–44.
- (41) Karki, R. G.; Kulkarni, V. M. A feature based pharmacophore for *Candida albicans* MyristoylCoA: protein N-myristoyltransferase inhibitors. *Eur. J. Med. Chem.* **2001**, *36*, 147–163.
- (42) Manetti, F.; Corelli, F.; Biava, M.; Fioravanti, R.; Porretta, G. C.; Botta, M. Building a pharmacophore model for a novel class of antitubercular compounds. *Farmaco* **2000**, *55*, 484–491.
- (43) Ekins, S.; Bravi, G.; Ring, B. J.; Gillespie, T. A.; Gillespie, J. S.; Vandenbranden, M.; Wrighton, S. A.; Wikel, J. H. Three-dimensional quantitative structure activity relationship analyses of substrates for CYP2B6. *J. Pharmacol. Exp. Ther.* **1999**, *288*, 21–29.
- (44) Ekins, S.; Bravi, G.; Binkley, S.; Gillespie, J. S.; Ring, B. J.; Wikel, J. H.; Wrighton, S. A. Three- and four-dimensional quantitative structure activity relationship analyses of cytochrome P-450 3A4 inhibitors. *J. Pharmacol. Exp. Ther.* **1999**, *290*, 429–438.

- (45) Ekins, S.; Bravi, G.; Binkley, S.; Gillespie, J. S.; Ring, B. J.; Wikel, J. H.; Wrighton, S. A. Three and four dimensional-quantitative structure activity relationship (3D/4D-QSAR) analyses of CYP2D6 inhibitors. *Pharmacogenetics* **1999**, *9*, 477–489.
- (46) Grigorov, M.; Weber, J.; Tronchet, J. M.; Jefford, C. W.; Milhous, W. K.; Maric, D. A QSAR study of the antimalarial activity of some synthetic 1,2,4-trioxanes. *J. Chem. Inf. Comput. Sci.* **1997**, *37*, 124–130.
- (47) Lopez-Rodriguez, M. L.; Porras, E.; Benhamu, B.; Ramos, J. A.; Morcillo, M. J.; Lavandera, J. L. First pharmacophoric hypothesis for 5-HT₇ antagonism. *Bioorg. Med. Chem. Lett.* **2000**, *10*, 1097–1100.
- (48) Daveu, C.; Bureau, R.; Baglin, I.; Prunier, H.; Lancelot, J. C.; Rault, S. Definition of a pharmacophore for partial agonists of serotonin 5-HT₃ receptors. *J. Chem. Inf. Comput. Sci.* **1999**, *39*, 362–369.
- (49) Norinder, U. Refinement of Catalyst hypotheses using simplex optimisation. *J. Comput. Aided Mol. Des.* **2000**, *14*, 545–557.
- (50) Bureau, R.; Daveu, C.; Baglin, I.; Sopkova-De Oliveira, S. J.; Lancelot, J. C.; Rault, S. Association of two 3D QSAR analyses. Application to the study of partial agonist serotonin-3 ligands. *J. Chem. Inf. Comput. Sci.* **2001**, *41*, 815–823.
- (51) Kurogi, Y.; Güner, O. F. Pharmacophore modeling and three-dimensional database searching for drug design using Catalyst. *Curr. Med. Chem.* **2001**, *8*, 1035–1055.
- (52) Güner, O. F.; Waldman, M.; Hoffman, R.; Kim, J.-H. Strategies for database mining and pharmacophore development. In *Pharmacophore Perception, Development, and Use in Drug Design*; Güner, O. F., Eds.; International University Line: La Jolla, CA, 2000; pp 213–236.
- (53) Langer, T.; Hoffman, R. D.; Bachmair, F.; Begle, S. Chemical function based pharmacophore models as suitable filters for 3D-database searching. *J. Mol. Struct.: THEOCHEM* **2000**, *500*, 59–72.
- (54) Kurogi, Y.; Miyata, K.; Okamura, T.; Hashimoto, K.; Tsutsumi, K.; Nasu, M.; Moriyasu, M. Discovery of novel mesangial cell proliferation inhibitors using a three-dimensional database searching method. *J. Med. Chem.* **2001**, *44*, 2304–2307.
- (55) Briens, F.; Bureau, R.; Rault, S. Applicability of CATALYST in ecotoxicology, a new promising tool for 3D-QSAR: study of chlorophenols. *Ecotoxicol. Environ. Saf.* **1999**, *43*, 241–251.
- (56) ChemDraw, version 6.0; CambridgeSoft Corporation: 100 Cambridge Park Drive, Cambridge, MA 02140, 2000.
- (57) Brooks, B. R.; Brucolleri, R. E.; Olafson, B. D.; States, D. J.; Swaminathan, S.; Karplus, M. CHARMM: A program for macromolecular energy minimization, and dynamic calculations. *J. Comput. Chem.* **1983**, *4*, 187–217.

JM010360C